Characterization of Protein Clusters of Diverse Magnetic Nanoparticles and Their Dynamic Interactions with Human Cells

ARTICLE *in* THE JOURNAL OF PHYSICAL CHEMISTRY C · MARCH 2009

Impact Factor: 4.77 · DOI: 10.1021/jp809493t

9 AUTHORS, INCLUDING:

Qingxin Mu
University of Washington Seattle
30 PUBLICATIONS **893** CITATIONS
SEE PROFILE

Sanjay R Mishra
The University of Memphis
168 PUBLICATIONS **1,588** CITATIONS
SEE PROFILE

Lei Yang
St. Jude Children's Research Hospital
21 PUBLICATIONS **331** CITATIONS
SEE PROFILE

Bing Yan
Shandong University
187 PUBLICATIONS **4,664** CITATIONS
SEE PROFILE

Characterization of Protein Clusters of Diverse Magnetic Nanoparticles and Their Dynamic Interactions with Human Cells

Qingxin Mu,[†,§,⊥] Zhenwei Li,[‡,⊥] Xi Li,[§] Sanjay R. Mishra,[∥] Bin Zhang,[‡] Zhikun Si,[‡] Lei Yang,[§] Wei Jiang,[‡] and Bing Yan*[,‡,§]

School of Pharmaceutical Sciences and School of Chemistry and Chemical Engineering, Shandong University, Jinan, Shandong 250100, People's Republic of China, St. Jude Children's Research Hospital, Memphis, Tennessee 38105, and The University of Memphis, Tennessee 38152

Received: October 27, 2008; Revised Manuscript Received: February 05, 2009

Although nanoparticle/protein binding and the cytotoxicity of nanoparticles have been separately reported, there has been no study linking the nature of nanoparticle/protein clusters to cell uptake and the dynamic cellular responses. We report here that water-soluble iron oxide-based magnetic nanoparticles (MNPs) with different sizes and surface chemistry bind different serum proteins in terms of protein identity and quantity without changing the protein secondary structures. Carboxylated MNPs (and aminated one in smaller MNPs) resulted in higher cytotoxicity, and PEG coating reduced both cell uptake and the cytotoxicity. Smaller MNPs (especially the carboxylated one) bind more serum proteins, are much less taken up by cells as compared to larger particles, and yet elicit more dynamic cytotoxic responses. Besides the intrinsic effects of size and surface charge of the water-soluble MNPs, the cellular effects of MNPs/protein clusters were also attributed to the identity and quantity of the adsorbed proteins rather than the binding-induced new epitopes on the proteins.

Introduction

Nanoparticles have been a research focus in various fields for a long time.[1−3] However, their biological effects have attracted wide societal and scientific concerns only in recent years.[4−6] Nanoparticles can be taken up by almost all species including mammals,[7] plants,[8] bacteria,[9] fungi,[10] and virus.[11] Nanoparticles have long been proposed to play an important role in future medicine.[12−14] The most advanced application of nanoparticles so far is the use of magnetic nanoparticles (MNPs) as MRI contrast agents.[14] Because of their large surface areas, nanoparticles have a strong tendency to bind biomolecules, such as proteins[15,16] and DNA,[17] in biological environment. Such bindings may be governed by the nanoparticle's structure, size, surface chemistry, and surface charge.[15,16,18,19] Interactions of nanoparticles with biomolecules such as proteins may interfere with the functions of both parties. For example, proteins adsorbed onto the nanoparticle surface may undergo conformational changes, leading to the exposure of new epitopes that may be accidentally recognized by signaling proteins and trigger signaling pathways.[20] On the other hand, nanoparticles with protein coating can be opsonized.[21] The nanoparticle/protein binding and the cytotoxic effects of nanoparticles have been separately studied and reported. However, very few studies tried to clarify the cellular effects of nanoparticle/protein clusters, which is the only existing form of nanoparticles in human cells.

In this investigation, we identified and quantified serum proteins bound to a group of soluble MNPs with various sizes and surface chemistry. Although commonly measured by end-point assays, cells always respond to nanoparticles in a time-dependent manner. Besides, highly soluble nanoparticles, including MNPs and other metal nanoparticles, when entering the human blood circulation system, are mainly excreted through the urinary system.[22] On the basis of this consideration, we selected a human embryonic kidney cell line (HEK293) as a research target to study dynamic cellular effects of diversified MNPs. Here, we monitored the dynamic cellular interactions between human cells (HEK293) and diverse MNP/proteins clusters using a real-time cell electronic sensing (RT-CES) assay.[23] Our results suggest that the size and surface chemistry of MNPs as well as the bound proteins regulate the cell uptake and the dynamic cellular responses. Because all MNPs studied here caused little conformational changes in the most abundant serum protein BSA, MNP-binding-induced conformational changes in bound proteins or exposed protein epitopes did not play a major role in cellular responses we observed.

Materials and Methods

Materials. Magnetic nanoparticles (∼200 and ∼50 nm; for dynamic light scattering data, see Supporting Information) with four different surface decorations (Figure 1) were purchased from Micromod Partikeltechnologie GmbH (Rostock-Warnemuende, Germany). Fetal bovine serum (FBS) was obtained from Invitrogen (Carlsbad, CA). Bovine serum albumin (BSA) was purchased from Bio Basic Inc. (Markham Ontario, Canada). HEK293 was obtained from ATCC (Rockville, MD). The Micro BCA (bicinchoninic acid) Protein Assay Kit was purchased from Pierce (Rockford, IL). The XTT kit was purchased from Roche Diagnostics GmbH (Mannheim, Germany). Guava Nexin Reagent and flow cytometer were purchased from Millipore (Billerica, MA).

Zeta Potential Measurement. The zeta potential of nanoparticles was determined using Zetasizer Nano-Z (Malvern Instruments, Worcestershire, UK). The analysis was performed

* Corresponding author. Phone: (901) 495-2797. Fax: (901) 495-5715. E-mail: bing.yan@stjude.org.
[†] School of Pharmaceutical Sciences, Shandong University.
[‡] School of Chemistry and Chemical Engineering, Shandong University.
[§] St. Jude Children's Research Hospital.
[∥] The University of Memphis.
[⊥] These authors contributed equally to this work.

10.1021/jp809493t CCC: $40.75
Published on Web 03/17/2009

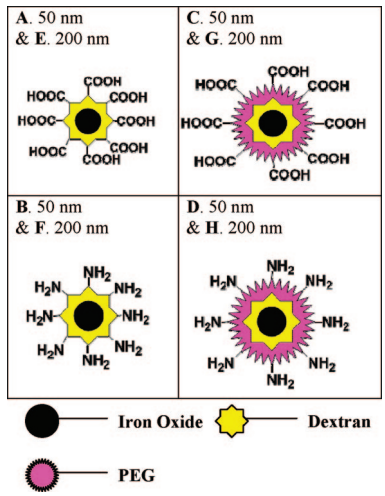

Figure 1. Cartoon representations of magnetic nanoparticles with different size and surface chemistry. (A−D) Iron oxide nanoparticles with a diameter of 50 nm. (E−H) Iron oxide nanoparticles with a diameter of 200 nm.

at 25.0 ± 0.2 °C using sample solutions in deionized distilled water or cell culture medium. The zeta potential was an average of three independent measurements.

Identification of Serum Proteins Bound to MNPs. For identification of proteins bound to various MNPs, the method was adapted from a previous report.[24] Briefly, MNPs solution was mixed with FBS and phosphate buffer saline (PBS) in 500 μL, and the final concentrations of MNPs and FBS were 2 mg/mL and 60%, respectively. Mixtures were incubated at 37 °C for 2 h. Next, the MNPs/protein clusters were isolated by centrifuge and washed four times (15 000*g*, 20 min). Proteins bound to MNPs surface were desorbed in SDS buffer, and the supernatant was collected after centrifugation. Protein solutions were analyzed with 10% SDS-PAGE. Gel was stained with Coomassie blue. Protein bands were identified by a MALDI-TOF/TOF analyzer (model 4700 Proteomics Analyzer from Applied Biosystems, Foster City, CA). Database searches were performed with Applied Biosystem's GPS explorer software, using the Mascot search engine. Protein assignments are made on the basis of both MS and MS/MS spectra. Swissprot (060108) was used for protein identification.

Quantification of Total Serum Protein Adsorption to MNPs. MNPs suspension was mixed with FBS in PBS (500 μL) in the same concentration as the previous section and incubated at 37 °C for 2 h. Next, the MNPs/protein clusters were isolated by centrifuge and washed four times (15 000*g*, 20 min). Proteins bound to MNPs surface were desorbed in 5% SDS and collected by centrifuge (15 000*g*, 20 min). The quantity of protein was determined by using a Micro BCA Protein Assay Kit.

Steady-State Fluorescence Spectroscopy of Serum Component BSA. Steady-state fluorescence spectra were measured using a Hitachi F-4500 spectrofluorometer (Hitachi Co. Ltd., Tokyo, Japan). Intrinsic fluorescence of proteins was measured by gradual addition of MNPs stock solutions. Final concentrations of MNPs in protein solutions were 0, 10, and 20 μg/mL, respectively. The concentration of all proteins was 20 μg/mL in PBS (pH ≈ 7.4). Proteins were excited at 280 nm, and the emission wavelength was set from 300 to 400 nm. Scanning speed was 1200 nm/min. Excitation and emission slit was set to 5.0 and 5.0 nm, respectively. PMT voltage was set to 700 V. Fluorescence intensities at 340 nm were used for calculation in the Stern−Volmer equation. All measurements were performed at 23 °C.

CD Spectroscopy of BSA. CD measurements were performed on a Jasco J-810 circular dichroism spectrometer (Jasco Co. Ltd., Tokyo). Concentrations of MNPs and proteins were the same as in the steady-state fluorescence assay. The spectra were measured between 190 and 250 nm with a bandwidth of 2.0 nm and a scan speed of 500 nm/min. Cuvette length was 10 mm. Three scans were averaged. All CD measurements were performed at 23 °C.

Transmission Electron Microscopic (TEM) Imaging of MNPs in Cells. HEK293 cells were treated with 100 μg/mL 200 nm MNP-D-COOH or MNP-D-NH_2 for 1 h. Next, cells were washed three times with PBS and fixed in 2.5% glutaraldehyde in 0.1 M sodium cacodylate buffer (pH 7.4) for 1 h at room temperature, then rinsed in three changes of same buffer. Cells were then post fixed 1 h in 2% osmium tetroxide with 3% potassium ferriocyanide, rinsed in three changes of the same buffer, then enbloc staining with a 2% aqueous uranyl acetate solution, and dehydration through a graded series of alcohol (50%, 70%, 80%, 95%, 100%). They were then put into two changes of propylene oxide, a series of propylene/Epon dilutions, and embedded. The thin (70 mμ) sections were cut on a Leica UC6 ultramicrotome, and images were taken on a JEOL 1200 EX (JEOL, Ltd. Tokyo, Japan) using an AMT 2k digital camera.

Determination of Cell Uptake of Various MNPs. MNPs solutions were added into HEK293 cell culture medium at a final concentration of [Fe] = 50 μg/mL. Twenty-four hours after MNPs addition, cell culture medium was drained and cells were washed three times with PBS buffer, and then harvested and resuspend in 0.5 mL of PBS buffer. The concentrations of Fe inside cell were determined using the QuantiChrom Iron Assay Kit (BioAssays Systems, Hayward, CA) in triplicate. The samples were extracted with 12 N HCl, neutralized with 10 N sodium hydroxide, and brought up to an appropriate volume. Quantification was carried out using a calibration curve generated from a set of standards. The linear detection range was 27−1000 μg/dL (4.8−179 μM), and the peak absorbance was measured at 590 nm.

Cell Cultures and Real-Time Cell-Based Electronic Sensing Assay (RT-CES). HEK293 cells were grown in Dulbecco's Minimum Essential Medium (DMEM, Gibco, Grand Island, NY) supplemented with 10% heat-inactivated fetal bovine serum, 2 mM L-glutamine, 100 μg/mL penicillin, and 100 U/mL streptomycin. The cells were grown in a humidified incubator at 37 °C (95% humidity, 5% CO_2). Multi E-Plate (MP) System (ACEA Biosciences, San Diego, CA) was used for the real-time cell-based electronic sensing assay. Six 96-well E-Plates were placed inside the MP station inside an incubator. The station was connected to the analyzer outside the incubator through a cable. The data were collected automatically by the electronic sensor analyzer under the control of MP software. The cell index (CI) is derived from the cell status-based cell-electrode impedance. The CI is calculated by eq 1:

$$\mathrm{CI} = \max_{i=1,\ldots,N}\left(\frac{R_{\mathrm{cell}}(fi)}{R_{\mathrm{b}}(fi)} - 1\right) \quad (1)$$

where $R_b(f)$ and $R_{cell}(f)$ are the frequency-dependent electrode resistances of background and cells, and N is the number of the frequency points at which the impedance is measured. The

TABLE 1: Zeta Potential of Nanoparticles in H_2O and Cell Culture Medium (pH 7.2)

size	letter	surface	zeta potential (mV)	
			H_2O	medium
50 nm	**A**	dextran-COOH	−31.6	−3.9
	B	dextran-NH_2	−11.4	−3.3
	C	dextran-PEG-COOH	−15.2	−3.8
	D	dextran-PEG-NH_2	−26.3	−4.7
200 nm	**E**	dextran-COOH	−39.4	−8.9
	F	dextran-NH_2	−11.8	−6.8
	G	dextran-PEG-COOH	−15.4	−9.6
	H	dextran-PEG-NH_2	−20.9	−8.6

CI reflects a gross condition of cell growth, such as cell number, cell adhesion, cell spreading, and cell morphological changes.

Volumes of 50 μL of media were added to wells in 96-well E-plates to obtain background readings followed by the addition of 100 μL of cell suspension (HEK293 10 000 cells per well). The cells were allowed to attach and spread on the sensors until the cell index reaches ~1.0 before adding MNPs. The data points were collected automatically every 15 min. Each concentration was triplicated.

Cell Proliferation (XTT) End Point Assay. Cell proliferation was performed by using an XTT assay. Cells were seeded in a 96-well microplate at a density of 6000 per well. MNPs were added to cells the next day at a final concentration of 100 μg/mL. Cells were allowed to grow 48 h after MNPs addition. Cells were then replaced with fresh medium to eliminate the influence of residue MNPs. XTT reagent was incubated with cells for 2 h at 37 °C followed by detection. Normalized cell proliferation was plotted on the basis of OD values measured. Each sample was triplicated.

Apoptosis Assay Using Flow Cytometry. Apoptotic or necrotic cells were stained with Annexin-V/PI and detected by flow cytometry. Cells were seeded in six-well microplate at a density of 20 000, and MNPs were added to cells the next day at a final concentration of 100 μg/mL. Cells were allowed to grow 48 h after MNPs addition. Cells were then trypsinized and aspirated. Guava Nexin Reagent was used for labeling of apoptotic or necrotic cells. Labeling and flow cytometry were performed under manufacturer's protocol. Each sample was duplicated.

Results and Discussion

The Profile of Serum Proteins Bound to MNPs Depends on Their Sizes and Surface Chemistry. Proteins bind to polymer nanoparticles,[24] MNPs,[25,26] and nanotubes.[15] The characteristics of clusters between serum proteins and MNPs were firmly established on the basis of three pieces of evidence. First, as compared to MNPs in water, the zeta potential of MNPs was up-shifted by 10−25 mV (Table 1) after incubation with cell culture medium that contained 10% fetal bovine serum. Proteins could bind to nanoparticles and change their surface potential. Similar changes have also been observed for gold nanoparticles[27] and a variety of other nanoparticles.[28] Second, after incubation of MNPs with bovine serum, proteins bound to MNPs were released and quantified by the spectrophotometric method (Figure 2c and d). These proteins were also separated and analyzed using gel electrophoresis (Figure 2a and b). We found that the same amount (weight) of MNPs of smaller sizes bound much more proteins as compared to larger particles. That was because the same mass of smaller MNPs possessed larger surface areas. When they were compared for bound proteins in the unit surface area, there were no differences (Figure 2c and d). Furthermore, MNP-COOH bound significantly more proteins as compared to other surface-modified MNPs. Third, surface-modified MNPs showed selectivity in protein binding (Figure 2a and b). Proteins selectively bound to each MNPs were identified by MALDI-TOF/TOF. The identified proteins are: (1) complement factor H; (2) vitronectin; (3) serum albumin; (4) α-1-antiproteinase; (5) complement C3; (6) thrombospondin-1; (7) complement C4; (8) mannose-binding protein C; (9) apolipoprotein A-1; (10) tetranectin; and (11) hemoglobin. Results demonstrated that, although some abundant proteins bound to all MNPs, protein binding was selective. Proteins 6, 7, and 9 only bound to MNP **A** and 8 to **B** and **D**. In summary, we have obtained compelling evidence that serum protein and MNPs formd clusters that contained different types of proteins each in different amount. Such bindings changed the global physiochemical properties of MNPs, such as surface potential. Protein clusters of MNPs with different sizes and different surface chemistry may have different cell uptake profiles and induce different cellular effects.

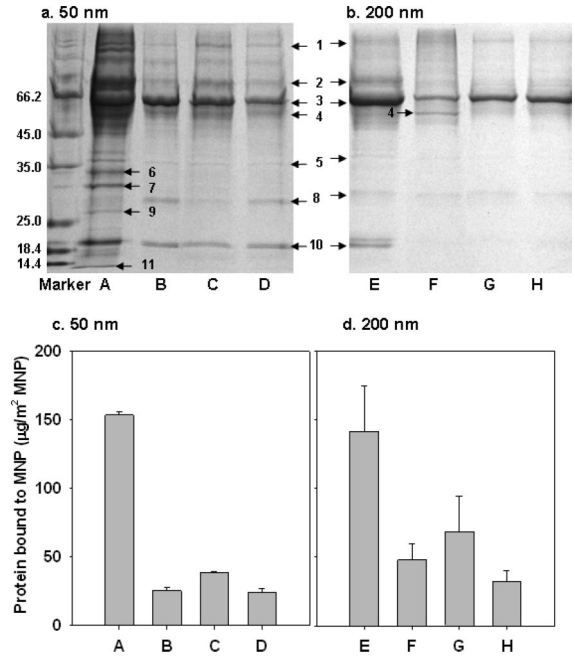

Figure 2. Serum protein adsorption of various MNPs. (a and b) Proteins selectively bound to each MNP were separated by electrophoresis and identified by MALDI-TOF/TOF MS. These proteins are: (1) complement factor H; (2) vitronectin; (3) serum albumin; (4) α-1-antiproteinase; (5) complement C3; (6) thrombospondin-1; (7) complement C4; (8) mannose-binding protein C; (9) apolipoprotein A-1; (10) tetranectin; (11) hemoglobin. (c and d) Quantification of adsorbed serum proteins onto various MNPs.

Serum Component Albumin Conserved Secondary Structure after Binding to MNPs. Protein conformation may be altered after binding to MNPs. This may expose new protein epitopes and potentially influence the cellular functions. To investigate whether MNP-bound serum proteins underwent conformational changes, we studied the binding between the major component of serum proteins, bovine serum albumin (BSA), and all MNPs using fluorescence and CD spectroscopy. Intrinsic fluorescence of proteins is sensitive to ligand binding. The quenching of protein intrinsic fluorescence indicates protein−ligand interactions.[29] The steady-state fluorescence of BSA was quenched by various MNPs (Figure 3a and b and Supporting Information). The results are consistent with findings in the previous section. Moreover, no shift in fluorescence emission peak was found in all MNPs (Supporting Information),

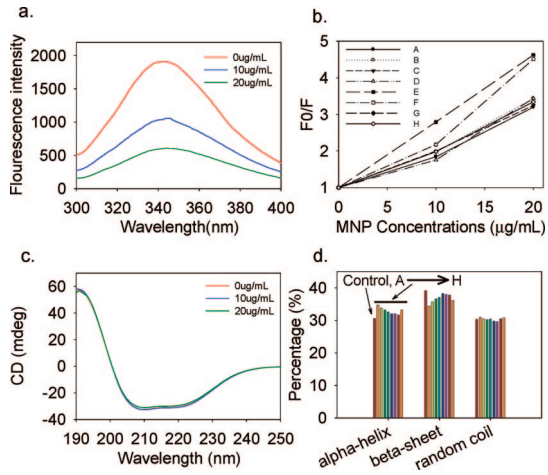

Figure 3. Steady-state fluorescence spectroscopy and CD spectra of BSA with MNPs titration. For fluorescence spectroscopy, BSA was dissolved in PBS at 20 μg/mL. MNPs stock solution was added to BSA solution to form final concentrations of 10 and 20 μg/mL, respectively. For CD, the experimental concentrations are the same as in fluorescence spectroscopy except that BSA was dissolved in dionized water. (a) Intrinsic fluorescence spectra of BSA before and after MNPs **A** titration; (b) ratio of initial fluorescence intensity (F_0) with modified BSA fluorescence intensity (F) at different concentrations of MNP. **A**−**H** are various MNPs with the same order as in Figure 1. (c) CD spectra of BSA before and after MNPs **A** titration; (d) BSA secondary structure calculation before and after 20 μg/mL MNPs addition using Yang formula.[41] The order of nanoparticles used is the same order as in Figure 1.

indicating that there were no changes in the environment of tryptophan residues as would happen in a global conformational change. To further investigate the influence of MNP-BSA binding on the protein's secondary structure, we measured CD spectra of BSA in the presence of various MNPs at the same concentrations as in the steady-state fluorescence spectroscopy measurements. Because protein structure is flexible and dynamic, we measured BSA secondary structures six times and observed a range of α-helixes (30.6−36.8%) and β-sheets (34.7−39.1%). As shown in Figure 3c and d, the protein's secondary structures with and without MNPs are in the range of normal BSA protein. As the most abundant protein in MNPs bound proteins, BSA might play a major role in affecting MNPs' cellular behavior, and its conformation was not changed by the presence of MNPs. Thus, we conclude that there is no change of secondary structure after being bound to MNPs. As a result, few protein epitopes should be exposed in MNP-bound proteins.

Relationship between Cell Uptake of MNPs with Nanoparticles' Size, Surface Chemistry, and Protein Binding. To study whether the different size and composition of MNP/protein clusters would change their cell uptake, we first imaged MNPs uptake using TEM (Figure 4). Images show that MNPs with carboxyl and amine decorations both entered cells in 1 h. Furthermore, both nanoparticles located into cytoplasmic vesicles, which indicates both nanoparticles were taken up into cells through endocytosis. Next, we quantitatively determined MNPs content that was taken up into cells by elemental (iron) analysis. As compared to the cell culture medium control, which is close to zero, different MNPs were internalized into cells in different quantities (Figure 5). Cells took up more large MNPs (**E**−**H**) than smaller ones (**A**−**D**). Studies on cell uptake of magnetic nanoparticles gave controversial results. Matuszewski et al. investigated the size effect on cell uptake and concluded that larger particles (65 nm) result in improved cell uptake over smaller ones (17 nm).[30] In another report, Thorek et al.

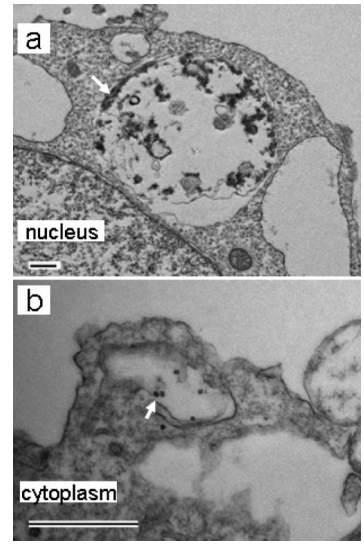

Figure 4. Transmission electron micrograph of MNPs **E** and **F** located in HEK293 cells 1 h after incubation; cells were treated with 100 μg/mL particles. MNPs were located in cytoplasmic vesicles. (a) 200 nm MNP-D-COOH (**E**); (b) 200 nm MNP-D-NH_2 (**F**). Arrows indicate MNPs. Scale bars represent 500 nm. Note that only the iron cores of MNPs are visible in the TEM.

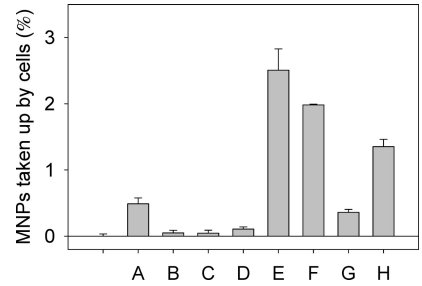

Figure 5. Percentage of MNPs taken up by HEK293 cells 24 h after nanoparticles addition. Cells were treated with MNPs as a concentration of [Fe] = 50 μg/mL.

concluded that performance of cell labeling reduced when particle size is greater than 200 nm.[31] Therefore, we carefully controlled surface modifications and size variations, and we applied various biophysical methods to characterize MNPs and their protein clusters. Higher protein binding by smaller MNPs might resist cell uptake. Furthermore, PEG coating reduced protein binding, and thus reduced cell uptake of MNPs with both carboxyl and amine decorations, which was consistent with a previous report.[32] From this study, it is clear that heavily clustered (smaller MNPs) or PEG-coated MNPs were less likely to be taken up by cells.

Real-Time Cell-Based Electronic Sensing Assay Reveals Dynamic Cellular Responses. Upon exposure to foreign materials, cells undergo time-dependent morphological and pathological changes. We measured dynamic cellular responses by RT-CES assay. This high-throughput assay is based on the parallel impedance measurement of attached cells using electronic sensors on the inner bottoms of wells in the 96-well electronic plate. The assay measures the real-time multiparameter index of cell growth named cell index (CI), which reflects the cell number, morphology, and attachment. This assay has been used in studying cellular responses to small molecules,[33] cells,[34] and environmental pollutant particles.[35] Here, for the first time, we applied this assay to investigate the cytotoxicity of nanoparticles.

MNPs alone did not generate any impedance signal, and the health status of cells was confirmed by the smooth rise of CI

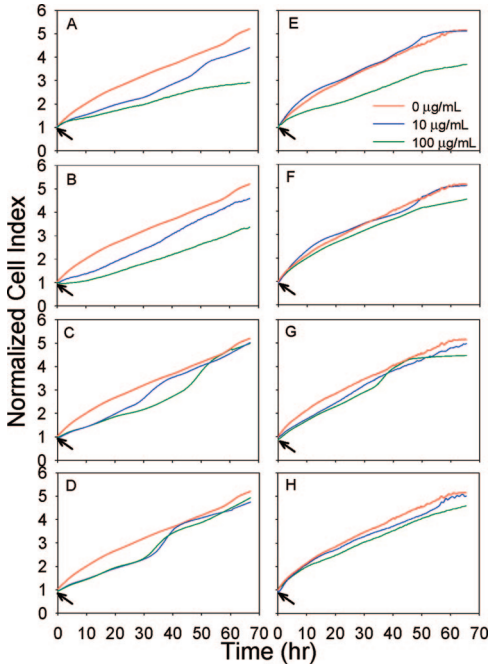

Figure 6. Real-time electronic sensoring of differential dynamic cellular responses of HEK293 cells to various MNPs/protein clusters. Nanoparticle concentrations are 0, 10, and 100 μg/mL, respectively. Cell index, which reflects the electric resistance of cell monolayer, is normalized to 1 at the time point at which MNPs were added. Time points at which nanoparticles were added are marked as arrows. The order of nanoparticles used is the same order as in Figure 1.

of nontreated cells with time (Figure 5). Cells were treated with nanoparticles when they entered the exponential growth phase (CI = 1.0). The moderate dose-dependent cell growth inhibition was only seen in cases of carboxylated MNPs **A** and **E** and smaller amine-functionalized MNPs **B**. Among MNPs with the same size, the nanoparticles funtionalized with −COOH (also with $-NH_2$ in smaller MNPs) are relatively more toxic (Figure 5, **A** and **E**). The MNPs with PEG component are relatively less toxic than those without PEG modification (Figure 5, **C**, **D**, **G**, **H** vs **A**, **B**, **E**, **F**). Smaller MNPs (50 nm) exhibited a slightly higher growth inhibition than did larger particles (200 nm) (see more inhibition in **B** vs **F** in Figure 4) even though the cell uptake of these MNPs was less. This indicated that the size, surface areas, or bound proteins may play a role in cytotoxicity. The surface carboxylated MNPs of either sizes induced more toxicity than amine-coated nanoparticles. Through our XTT assay,[36] the MNPs have the same pattern with RT-CES on cell proliferation (Figure 6a). Besides, all MNPs do not induce cell apoptosis or necrosis as compared to medium control (Figure 6b). These real-time assay and end point results agree with the existing reports of toxicity studies on MNPs.[32,37,38]

Dynamic Cellular Response Is Governed by Combined Effects of MNPs' Size, Surface Chemistry, and the Identity and Quantity of Bound Proteins. This study aimed to understand how protein binding to nanoparticles influences their dynamic cellular impacts. We were especially interested in understanding the combined effects of MNP itself and the identity, quantity, and conformational integrity of the bound proteins on cell uptake and cytotoxicity.

By diversifying the size and surface chemistry of MNPs, we found that they bound to different proteins in different amount and induced diverse cell uptake and different dynamic cellular responses. We report four major findings: (1) MNPs with smaller size and negative charges bound more serum proteins, probably

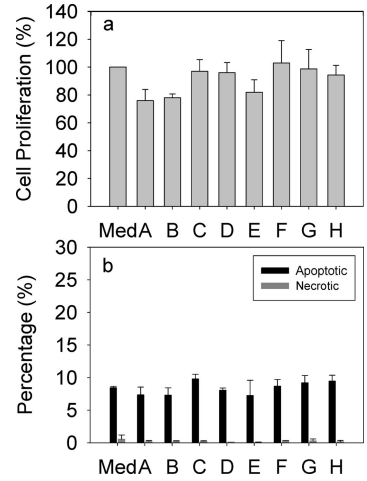

Figure 7. Cell proliferation and apoptosis end point assays. (a) Cell proliferation percentage of HEK293 incubated with MNPs for 48 h. Control (Med) was normalized to 100. (b) Percentages of apoptotic and necrotic cells in total cell culture with (**A**−**H**, 48 h) and without (Med) MNPs.

due to their large surface areas and the increased electrostatic interactions. (2) MNPs might not change the conformation of bound proteins because the major bound protein BSA molecules maintained their secondary structure after MNP binding. This may be due to the hydrophilic nature of MNPs. It should be noted that more hydrophobic nanoparticles, such as nanotubes, caused detectable changes in protein secondary structures.[15] (3) The prior PEG modification or the in situ protein clustering both reduced cell uptake of MNPs. (4) Diverse MNPs/proteins clusters induced different dynamic cytotoxicity. Smaller MNPs, although heavily clustered by proteins and less taken up by cells, showed more cytotoxicity as compared to larger MNPs. Carboxylated MNPs of either sizes also showed more cytotoxicity.

Concluding Remarks

Although nanoparticle/protein binding and nanoparticles' cytotoxicity have been separately reported, there has been no study linking the nature of nanoparticle/protein clusters to cell uptake and dynamic cellular responses. We report here that MNPs with different sizes and surface chemistry bound different serum proteins in terms of protein identity and quantity without changing the protein secondary structure. Different MNPs bind different patterns of serum proteins and elicited different dynamic cellular responses. Besides the intrinsic effects of size and surface chemistry of MNPs, the cellular effects of MNPs/protein clusters were most likely due to the identity and quantity of the adsorbed proteins rather than the induced epitopes from protein conformational changes. Identified MNPs/protein clusters help us further understand the intercellular and intracellular behaviors of nanomaterials. The conserved protein conformation in NP/protein clusters can be further exploited for protein cellular transportation and the targeted delivery of protein therapeutics.[39,40] Based on this study, the influence of nanoparticle/protein clusters on cellular physiological processes, such as signaling transduction, should be further studied.

Acknowledgment. This work was supported by National Basic Research Program of China (973 Program 2009CB930103), the American Lebanese and Syrian Associated Charities (ALSAC), and St. Jude Children's Research Hospital.

Supporting Information Available: Details of the dynamic light scattering characterization (DLS) and transmission electron

micrographs (TEM) of MNPs, and protein binding studies using steady-state fluorescence spectroscopy and circular dichroism. This material is available free of charge via the Internet at http://pubs.acs.org.

References and Notes

(1) Michalet, X.; Pinaud, F. F.; Bentolila, L. A.; Tsay, J. M.; Doose, S.; Li, J. J.; Sundaresan, G.; Wu, A. M.; Gambhir, S. S.; Weiss, S. *Science* **2005**, *307*, 538–544.

(2) Tans, S. J.; Devoret, M. H.; Dai, H. J.; Thess, A.; Smalley, R. E.; Geerligs, L. J.; Dekker, C. *Nature* **1997**, *386*, 474–477.

(3) Vogel, E. M. *Nat. Nanotechnol.* **2007**, *2*, 25–32.

(4) Service, R. F. *Science* **2004**, *304*, 1732–1734.

(5) Maynard, A. D.; Aitken, R. J.; Butz, T.; Colvin, V.; Donaldson, K.; Oberdorster, G.; Philbert, M. A.; Ryan, J.; Seaton, A.; Stone, V.; Tinkle, S. S.; Tran, L.; Walker, N. J.; Warheit, D. B. *Nature* **2006**, *444*, 267–269.

(6) Nel, A.; Xia, T.; Madler, L.; Li, N. *Science* **2006**, *311*, 622–627.

(7) Lam, C. W.; James, J. T.; McCluskey, R.; Hunter, R. L. *Toxicol. Sci.* **2004**, *77*, 126–134.

(8) Lin, D. H.; Xing, B. S. *Environ. Sci. Technol.* **2008**, *42*, 5580–5585.

(9) Kloepfer, J. A.; Mielke, R. E.; Nadeau, J. L. *Appl. Environ. Microbiol.* **2005**, *71*, 2548–2557.

(10) Navarro, E.; Baun, A.; Behra, R.; Hartmann, N. B.; Filser, J.; Miao, A. J.; Quigg, A.; Santschi, P. H.; Sigg, L. *Ecotoxicology* **2008**, *17*, 372–386.

(11) Lu, L.; Sun, R. W. Y.; Chen, R.; Hui, C. K.; Ho, C. M.; Luk, J. M.; Lau, G. K. K.; Che, C. M. *Antiviral Ther.* **2008**, *13*, 253–262.

(12) Rabin, O.; Perez, J. M.; Grimm, J.; Wojtkiewicz, G.; Weissleder, R. *Nat. Mater.* **2006**, *5*, 118–122.

(13) Reddy, S. T.; van der Vlies, A. J.; Simeoni, E.; Angeli, V.; Randolph, G. J.; O'Neill, C. P.; Lee, L. K.; Swartz, M. A.; Hubbell, J. A. *Nat. Biotechnol.* **2007**, *25*, 1159–1164.

(14) Lee, J. H.; Huh, Y. M.; Jun, Y.; Seo, J.; Jang, J.; Song, H. T.; Kim, S.; Cho, E. J.; Yoon, H. G.; Suh, J. S.; Cheon, J. *Nat. Med.* **2007**, *13*, 95–99.

(15) Mu, Q.; Liu, W.; Xing, Y.; Zhou, H.; Li, Z.; Zhang, Y.; Ji, L.; Wang, F.; Si, Z.; Zhang, B.; Yan, B. *J. Phys. Chem. C* **2008**, *112*, 3300–3307.

(16) Zhou, H.; Mu, Q.; Gao, N.; Liu, A.; Xing, Y.; Gao, S.; Zhang, Q.; Qu, G.; Chen, Y.; Liu, G.; Zhang, B.; Yan, B. *Nano Lett.* **2008**, *8*, 859–865.

(17) Li, X.; Peng, Y. H.; Ren, J. S.; Qu, X. G. *Proc. Natl. Acad. Sci. U.S.A.* **2006**, *103*, 19658–19663.

(18) Shang, W.; Nuffer, J. H.; Dordick, J. S.; Siegel, R. W. *Nano Lett.* **2007**, *7*, 1991–1995.

(19) Lundqvist, M.; Sethson, I.; Jonsson, B. H. *Langmuir* **2004**, *20*, 10639–10647.

(20) Lynch, I.; Dawson, K. A.; Linse, S. *Sci. Signal.* **2006**, *2006*, pe14.

(21) Owens, D. E.; Peppas, N. A. *Int. J. Pharm.* **2006**, *307*, 93–102.

(22) Jain, T. K.; Reddy, M. K.; Morales, M. A.; Leslie-Pelecky, D. L.; Labhasetwar, V. *Mol. Pharm.* **2008**, *5*, 316–327.

(23) Solly, K.; Wang, X. B.; Xu, X.; Strulovici, B.; Zheng, W. *Assay Drug Dev. Tech.* **2004**, *2*, 363–372.

(24) Cedervall, T.; Lynch, I.; Lindman, S.; Berggard, T.; Thulin, E.; Nilsson, H.; Dawson, K. A.; Linse, S. *Proc. Natl. Acad. Sci. U.S.A.* **2007**, *104*, 2050–2055.

(25) Peng, Z. G.; Hidajat, K.; Uddin, M. S. *J. Colloid Interface Sci.* **2004**, *271*, 277–283.

(26) Macaroff, P. P.; Simioni, A. R.; Lacava, Z. G. M.; Lima, E. C. D.; Morais, P. C.; Tedesco, A. C. *J. Appl. Phys.* **2006**, *99*, 3.

(27) Jiang, W.; Kim, B. Y. S.; Rutka, J. T.; Chan, W. C. W. *Nat. Nanotechnol.* **2008**, *3*, 145–150.

(28) Xia, T.; Kovochich, M.; Brant, J.; Hotze, M.; Sempf, J.; Oberley, T.; Sioutas, C.; Yeh, J. I.; Wiesner, M. R.; Nel, A. E. *Nano Lett.* **2006**, *6*, 1794–1807.

(29) Gratton, E.; Jameson, D. M.; Hall, R. D. *Annu. Rev. Biophys. Bioeng.* **1984**, *13*, 105–124.

(30) Matuszewski, L.; Persigehl, T.; Wall, A.; Schwindt, W.; Tombach, B.; Fobker, M.; Poremba, C.; Ebert, W.; Heindel, W.; Bremer, C. *Radiology* **2005**, *235*, 155–61.

(31) Thorek, D. L. J.; Tsourkas, A. *Biomaterials* **2008**, *29*, 3583–3590.

(32) Hu, F. X.; Neoh, K. G.; Cen, L.; Kang, E. T. *Biomacromolecules* **2006**, *7*, 809–816.

(33) Xing, J. Z.; Zhu, L. J.; Jackson, J. A.; Gabos, S.; Sun, X. J.; Wang, X. B.; Xu, X. *Chem. Res. Toxicol.* **2005**, *18*, 154–161.

(34) Zhu, J.; Wang, X. B.; Xu, X.; Abassi, Y. A. *J. Immunol. Methods* **2006**, *309*, 25–33.

(35) Huang, L.; Xie, L.; Boyd, J. M.; Li, X. F. *Analyst* **2008**, *133*, 643–648.

(36) Roehm, N. W.; Rodgers, G. H.; Hatfield, S. M.; Glasebrook, A. L. *J. Immunol. Methods* **1991**, *142*, 257–265.

(37) Berry, C. C.; Wells, S.; Charles, S.; Aitchison, G.; Curtis, A. S. G. *Biomaterials* **2004**, *25*, 5405–5413.

(38) Muller, K.; Skepper, J. N.; Posfai, M.; Trivedi, R.; Howarth, S.; Corot, C.; Lancelot, E.; Thompson, P. W.; Brown, A. P.; Gillard, J. H. *Biomaterials* **2007**, *28*, 1629–1642.

(39) Kam, N. W. S.; Liu, Z. A.; Dai, H. J. *Angew. Chem., Int. Ed.* **2006**, *45*, 577–581.

(40) Li, Y. P.; Pei, Y. Y.; Zhang, X. Y.; Gu, Z. H.; Zhou, Z. H.; Yuan, W. F.; Zhou, J. J.; Zhu, J. H.; Gao, X. J. *J. Controlled Release* **2001**, *71*, 203–211.

(41) Yang, J. T.; Wu, C. S. C.; Martinez, H. M. *Methods Enzymol.* **1986**, *130*, 208–269.

JP809493T